

## Miscibility of Poly(*n*-butyl acrylate)/Poly(propylene glycol) Blends. 2. Dielectric Study of Local Heterogeneity

Tadashi Hayakawa<sup>†</sup> and Keiichiro Adachi\*

Department of Macromolecular Science, Graduate School of Science, Osaka University, Toyonaka, Osaka 560-0043, Japan

Received April 19, 2000

**ABSTRACT:** Dielectric measurements were carried out on blends composed of poly(*n*-butyl acrylate) (PBA) and poly(propylene glycol) (PPG) exhibiting phase behavior of the UCST type. Both linear PPG and three-arm star-shaped PPG were used. The frequency dependence curves of the dielectric loss factor  $\epsilon''$  exhibited a main peak due to segmental motions and a shoulder due to the normal mode relaxation of the PPG molecules. Depending on the difference between the cloud point  $T_{\text{cloud}}$  and temperatures of dielectric measurements  $T_{\text{meas}}$ , the shape of the  $\epsilon''$  curves changed. The observed  $\epsilon''$  curves were compared with theoretical  $\epsilon''$  curves calculated on the basis of mixing rules for the completely mixed and demixed states. It was found that when  $T_{\text{meas}} \sim T_{\text{cloud}}$ , the  $\epsilon''$  curves exhibited relaxation spectra intermediate to the theoretical curves for the mixed and demixed states. This indicates that the PBA and PPG segments are not perfectly mixed even at temperatures above the cloud point. The main peak was broader than those of the components, but the peak for the normal mode did not exhibit broadening, indicating that the correlation length of the heterogeneity is less than the end-to-end distance of the PPG molecules. A Gaussian distribution of the local concentration can be deduced from the  $\epsilon''$  curves. Dielectric behavior of blends containing star-shaped PPG was found to be similar to those with linear PPG.

### Introduction

In part 1 of this series of study, we reported the cloud points, glass transition temperatures  $T_g$ , and dielectric behavior for blends composed of poly(*n*-butyl acrylate)-PBA/linear poly(propylene glycol) (PPGD) and PBA/star-shaped poly(propylene glycol) with three arms (PPGT).<sup>1</sup> It was found that the phase diagrams of these blends are of the UCST type, and the interaction parameter  $\chi$  calculated on the basis of the mean-field theory by Flory and Huggins<sup>2,3</sup> for blends composed of a linear PPG is different from that based on star-shaped PPG. This apparent difference of  $\chi$  was explained by assuming screening of the PBA segments at the center of the star-shaped PPG molecules. However, no evidence of such an internal segregation was found in either differential scanning calorimetry or the temperature dependence of dielectric loss for blends of star-shaped PPG.<sup>1</sup> For blends having a cloud point near the temperatures of the dielectric measurements, it was observed that although the blends exhibited a single  $T_g$ , the temperature dependence of the dielectric loss was bimodal. In this paper we examine the dielectric behavior of PBA/PPG blends in the frequency plane, focusing our attention on the difference between linear and star-shaped PPG.

Previously, Se et al. reported a dielectric study of miscibility for blends composed of *cis*-polyisoprene (*cis*-PI) and low molecular weight polystyrene (PS) and for blends of *cis*-PI and vinylpolyisoprene (vinyl-PI).<sup>4</sup> It is known that *cis*-PI is a type A polymer having a component of dipole moment aligned parallel to the chain contour and exhibiting a dielectric normal mode relaxation reflecting the fluctuation of the end-to-end vector.<sup>5,6</sup> On the other hand, PS and vinyl-PI possess

only the perpendicular component (type B) and exhibit the primary ( $\alpha$ ) relaxation due to local segmental motions. Se et al.<sup>4</sup> argued that if a blend is composed of a polymer having both type A and type B dipoles, the dielectric behavior of the normal mode and the segmental mode reflects the miscibility in the length scale of the end-to-end distance (2–100 nm) and the length scale of the monomeric units (0.1–1 nm), respectively. They concluded that there exists a heterogeneity of the length scale of the order of the size of the segment in blends of *cis*-PI/PS and *cis*-PI/vinyl-PI. In the present blend, PPG is a type A polymer,<sup>7,8</sup> but PBA is a type B polymer. On the basis of this view, we have examined the dielectric behavior of the segmental and normal modes of PPG in the present blends.

Recently, several authors investigated the local heterogeneity in miscible polymer blends and found that a local heterogeneity results in a broader distribution of dielectric relaxation times.<sup>9–13</sup> Shears and Williams observed first that dielectric relaxation spectra are broadened by concentration fluctuations in low molecular weight liquids.<sup>14</sup> Katana et al.<sup>10</sup> reported the effects of concentration fluctuation on the dielectric primary relaxation for a polymer blend composed of poly(cyclohexyl acrylate-*stat*-butyl methacrylate) and polystyrene. They explained the relaxation spectrum by assuming a Gaussian distribution of the local heterogeneity, based on the model proposed by Zetsche and Fischer.<sup>9</sup> The amplitude of this heterogeneity is expected to increase in the temperature range near the phase-separation temperature. On the basis of the phase diagram reported in part 1, we examine the dielectric behavior near the cloud point.

### Theory

For analyses of dielectric data of a polymer blend composed of components 1 and 2, it is necessary to express the complex dielectric constant  $\epsilon_b^*$  of the blend

<sup>†</sup> Present address: Nippon NSC Co., 1-6-5 Senba-nishi, Minou-shi, Osaka 562-8586, Japan.

\* To whom correspondence should be addressed.

as a function of the complex dielectric constant  $\epsilon_j^*$  of the components and the composition  $w_j$  ( $j = 1$  and  $2$ ). First we consider the dielectric response of a blend in which the components are completely demixed. When the concentration  $w$  (w/v) of either component is small and the domains are spherical or ellipsoidal,  $\epsilon_b^*$  is expressed by the Wagner and Sillars theory.<sup>15,16</sup> When the  $w_j$  of the components are comparable,  $\epsilon_b^*$  is a function of the morphology as well as composition. Unfortunately, the theory of the dependence of  $\epsilon_b^*$  on morphology is not available. Therefore, we use  $\epsilon_b^*$  calculated for two simple cases where the domains are oriented in the direction either parallel or perpendicular to the electrodes. In the case of perpendicular orientation,  $\epsilon_b^*$  is given simply by the weighted sum of  $\epsilon_j^*$  of the components 1 and 2

$$\epsilon_b^*(\omega) = w_1\epsilon_1^*(\omega) + w_2\epsilon_2^*(\omega) \quad (1)$$

In the case of parallel orientation, the  $\epsilon^*$  is given by

$$\frac{1}{\epsilon_b^*(\omega)} = \frac{w_1}{\epsilon_1^*(\omega)} + \frac{w_2}{\epsilon_2^*(\omega)} \quad (2)$$

When  $\epsilon_1^*$  and  $\epsilon_2^*$  are of the same order, numerical calculation with eq 2 indicates that the real and imaginary parts of  $\epsilon_b^*$  change almost linearly with  $w$ . Therefore, eq 1 is a good approximation for the demixed state, and we use eq 1 as a mixing rule for demixed blends.

For a miscible blend,  $\epsilon_b^*$  depends on both the effective dipole moments  $\mu_{\text{eff}}$  and the relaxation times of the components. Generally the square of  $\mu_{\text{eff}}$  is proportional to the internal field factor  $F$  and the dipolar correlation factor  $g$  proposed by Kirkwood;<sup>17–19</sup> i.e.,  $\mu_{\text{eff}}^2 = gu^2F$  where  $\mu$  is the dipole moment in a vacuum. It is reported<sup>20</sup> that  $g$  of polymers is mainly due to the intramolecular interactions, and therefore we expect that  $g$  does not change appreciably by blending, as reported by Wetton et al.<sup>13</sup> The factor  $F$  is a function of the relaxed and unrelaxed dielectric constants.<sup>18</sup> If the dielectric constants of the components of a blend are similar,  $F$  should not change greatly by blending. Thus, we will use a miscibility rule in which the changes of  $g$  and  $F$  are not taken into account.

The relaxation times of the components vary so that the molecules 1 and 2 move under a common frictional drag  $\zeta_b$  in the blend. This phenomenon is known for mixtures of low molecular weight substances<sup>14,21,22</sup> and for polymers.<sup>11,23</sup> Then the relaxation time  $\tau_j$  of the component  $j$  changes from  $\tau_j$  in the pure state to  $\tau_j\zeta_b/\zeta_j$  by mixing, and hence, the  $\epsilon''$  curves of the components shift along the axis of angular frequency  $\omega$  correspondingly. Thus, if the complex dielectric constants of the components are denoted as  $\epsilon_j^*(\omega)$ ,  $\epsilon_b^*(\omega)$  is given by

$$\epsilon_b^*(\omega) = w_1\epsilon_1^*(\omega\zeta_b/\zeta_1) + w_2\epsilon_2^*(\omega\zeta_b/\zeta_2) \quad (3)$$

It is known for mixtures of low molecular weight substances that this equation holds only when dielectric measurements are carried out in the audio frequency range and at temperatures near  $T_g$ , where the molecules move cooperatively.<sup>14,22</sup> At high temperatures corresponding to a frequency range above 10 MHz, the components tend to move independently at different rates, and hence eq 3 does not hold.<sup>22</sup> The experimental window employed in the present study satisfies the

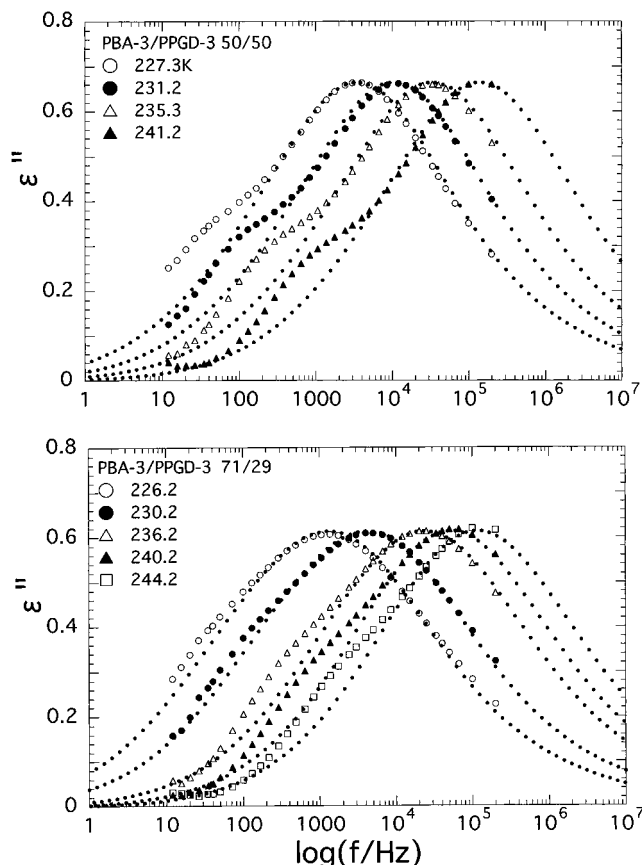


**Figure 1.** Frequency  $f$  dependence of dielectric loss factor  $\epsilon''$  for blends of PBA-3/PPGD-3. Top figure is for a blend of PBA/PPGD-3 which is 50/50 (by weight) and bottom for 71/29.

above condition. Thus, eq 3 can be regarded as a mixing rule for completely miscible states.

## Experimental Section

The samples used in this study have been described in part 1.<sup>1</sup> The figures of the sample code indicate the weight-average molecular weight in units of  $\text{kg mol}^{-1}$ . For example, PBA-380 indicates poly(*n*-butyl acrylate) with the weight-average molecular weight  $M_w = 3.8 \times 10^5$ . Linear PPG with  $M_w = 3.0 \times 10^3$  is coded as PPGD-3 and three-arm star-shaped PPG with  $M_w = 5.9 \times 10^3$  as PPGT-6. Blends are coded in such a way as PBA-21/PPGD-3 (50/50), which indicates that the blend is composed of PBA-21 and PPGD-3 with the mixing ratio of 50/50 by weight. Concentration  $w$  in w/v was calculated with the density  $\rho$  of PBA and PPG:<sup>24</sup>  $\rho_{\text{PBA}} = 1.087$  and  $\rho_{\text{PPG}} = 0.998$ . Dielectric measurements were carried out with an RLC digibridge (QuadTech 1693, Maynard, MA) in the frequency range from 12 Hz to 200 kHz. All samples were loaded in a dielectric cell at room temperature and cooled at the rate of ca. 3 K/min.

## Results and Discussion

**Dielectric Behavior of PBA/PPG Blends.** As reported in part 1, the dielectric relaxations of PBA/PPG blends were observed in the temperature range from 210 to 250 K in our experimental window from 12 Hz to 200 kHz. Depending on the cloud point relative to the temperature of dielectric measurements, the blend exhibited dielectric behavior characteristic of either the mixed or demixed states. Figures 1, 2, and 3 show representative frequency ( $f$ ) dependence curves of dielectric loss factor  $\epsilon''$  for PBA-3/PPGD-3(50/50 and 71/29), PBA-21/PPGD-3(50/50 and 65/35), and PBA-380/PPGT-6(50/50), respectively. The first blend of PBA-3/

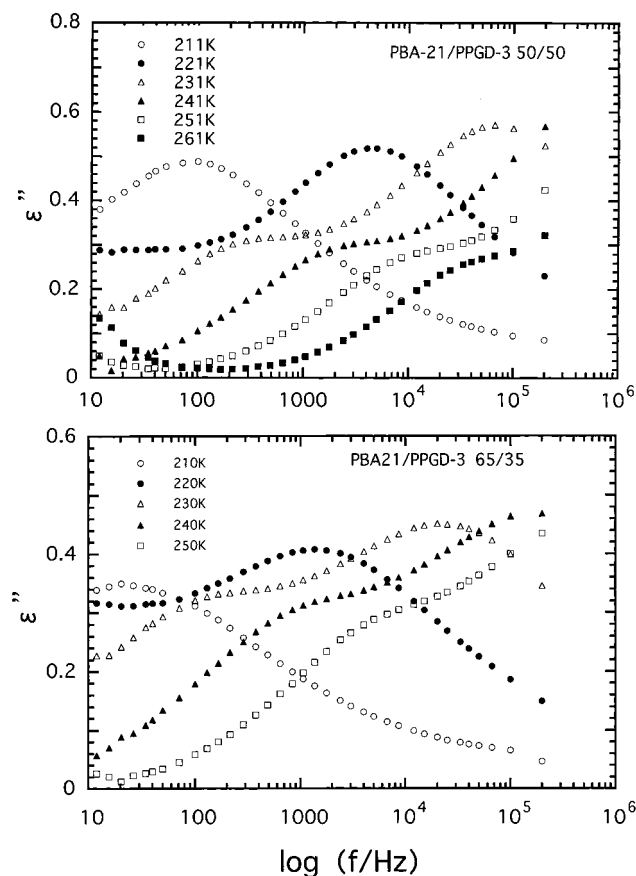


**Figure 2.** Frequency  $f$  dependence of dielectric loss factor  $\epsilon''$  for blends of PBA-21/PPGD-3 at various temperatures given in the figure. Top graph is for a blend of PBA/PPGD-3 which is 50/50 (by weight) and bottom for 65/35.

PPGD-3 is in the mixed state, exhibiting a main peak and a small shoulder due to the normal mode of PPG in the low-frequency side. The dotted line in Figure 1 indicates eq 7 to be discussed later. On the other hand, the third blend of PBA-380/PPGT-6 is a demixed blend and exhibits two well-resolved peaks. The second blend PBA-21/PPGD-3 has cloud point close to temperatures of dielectric measurements. Although not shown here, PBA-21/PPGT-6 exhibited  $\epsilon''$  curves very similar to those shown in Figure 2. No clear change can be seen in the  $\epsilon''$  curves at the cloud point 240 K for the 50/50 composition and 228 K for 65/35 composition which have been estimated in part 1.<sup>1</sup> The  $\epsilon''$  curves for PBA-21/PPGD-3 and PBA-21/PPGT-6 exhibit a spectrum intermediate between the  $\epsilon''$  curves for the mixed and demixed states. We will analyze this behavior using the blending rules given by eqs 1 and 3.

For calculation of  $\epsilon''$  of blends with the mixing rules given by eqs 1 and 3, we need  $\epsilon''$  for pure PBA and PPG. As in many amorphous polymers, the  $\epsilon''$  curves of PBA and PPG measured at different temperatures were superposable within experimental error.<sup>7</sup> The master curves of  $\epsilon''$  for pure PBA samples are shown in Figure 4. The curves were fitted to the Havriliak–Negami equation<sup>25</sup> for analyses of the blend data:

$$\epsilon' - i\epsilon'' = \frac{\Delta\epsilon}{[1 + (i\omega\tau_0)^\alpha]^\beta} + \epsilon_u \quad (4)$$

where  $\epsilon_u$  is the unrelaxed dielectric constant,  $\Delta\epsilon$  is the

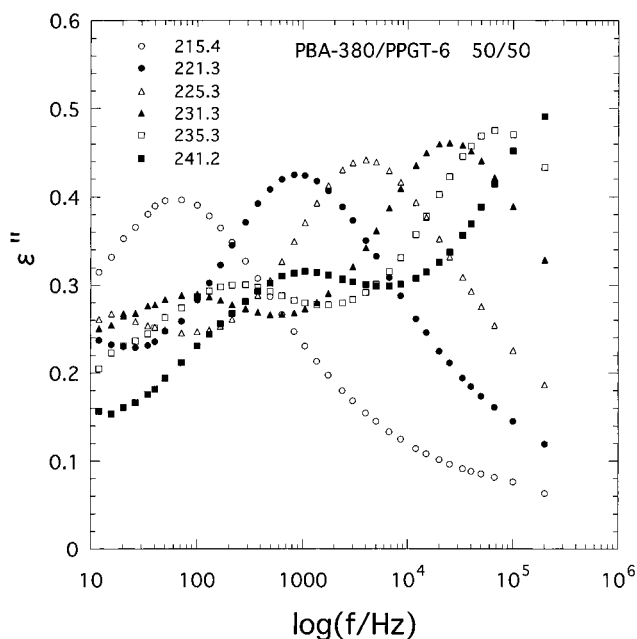


**Figure 3.** Frequency  $f$  dependence of dielectric loss factor  $\epsilon''$  for a blend of PBA-380/PPGT-6(50/50).

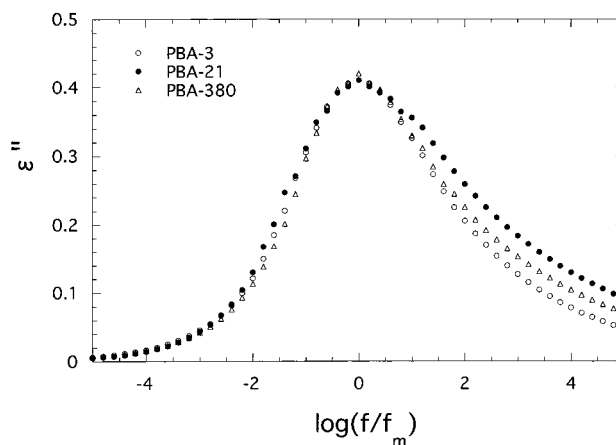


**Figure 4.** Master curves of  $\epsilon''$  for PBA-3, PBA-21, and PBA-380 used in this study. Here  $f_m$  denotes the loss maximum frequency given in Figures 10 and 15.

**Table 1. Exponents of the Havriliak–Negami Equation**

code	$\alpha$	$\beta$
PBA-3	0.43	0.53
PBA-21	0.45	0.31
PBA-380	0.43	0.51
PPGD-3	0.55	0.66
PPGT-6	0.55	0.66

relaxation strength, and  $\alpha$  and  $\beta$  are parameters. The parameters  $\alpha$  and  $\beta$  for PBA and PPG samples are listed in Table 1.

Figure 5 shows the master curve of  $\epsilon''$  for linear PPGD-3. The  $\epsilon''$  for star-shaped PPGT-6 is very similar to PPGD-3. The normal mode relaxation is seen as a shoulder in the low-frequency side.<sup>7,8</sup> The main peak due to the segmental mode was fitted to the Havriliak–Negami equation, and the contribution of the segmental mode on the low-frequency side of the loss peak was estimated as shown in this figure. The contribution of the normal mode thus resolved will be used to examine the behavior of the normal mode in blends. Figure 6 shows the  $\epsilon''$  curves calculated with eq 3 for miscible PBA-3/PPGD-3 blends. Frequency is normalized by the

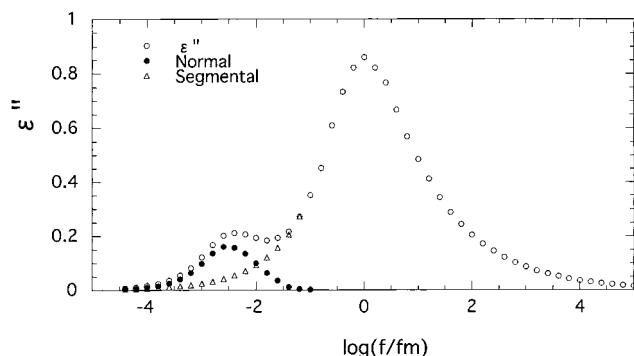


**Figure 5.** Master curves of  $\epsilon''$  for PPGD-3. Open circle, closed circle, and triangle keys indicate the observed  $\epsilon''$  curve, the contribution of the normal mode, and the  $\epsilon''$  curve from which the contribution of the normal mode is subtracted. Here  $f_m$  denotes the loss maximum frequency given in Figure 10.

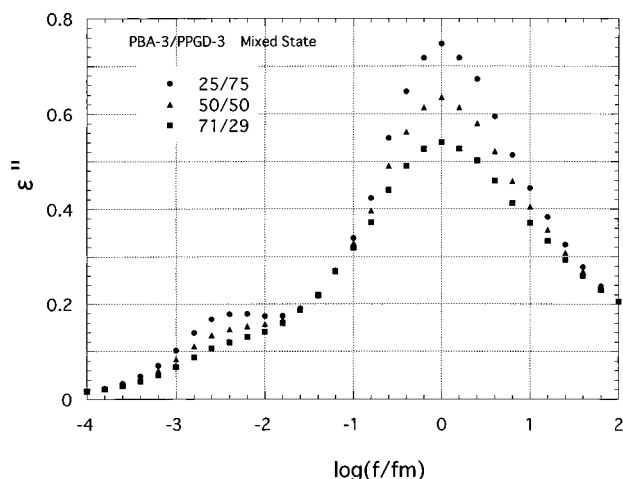


**Figure 6.** Theoretical  $\epsilon''$  curves calculated with eq 3 for mixed blends of PBA-3/PPGD-3. Calculations were made with the master curves shown in Figures 4 and 5.

loss maximum frequency  $f_m$  of the main peak. For the other blends, the theoretical  $\epsilon''$  curves calculated with eq 3 are very similar to those shown in this figure.

**Dielectric Behavior of Miscible Blends.** In this section we analyze the data for miscible blends composed of PBA-3 and either PPGD-3 or PPGT-6. First we attempted to resolve the  $\epsilon''$  curves (denoted as  $\epsilon''_b$ ) of those blends into the contributions of the normal mode and the segmental mode. The  $\epsilon''$  curve for the normal mode ( $\epsilon''_{nm}$ ) estimated in Figure 5 was multiplied by the PPG content  $w_{PPG}$ , and then  $w_{PPG}\epsilon''_{nm}$  was subtracted from  $\epsilon''_b$  as shown in Figures 7 and 8. As is seen in these figures, the  $\epsilon''$  curves after subtraction of the contribution of the normal mode is smooth, indicating that the relaxation spectrum for the normal mode does not change in blends.

In Figures 7 and 8, we note that the observed main peak is broader than the calculated one shown in Figure 6. For example, the half-width of PBA-3/PPGD-3(50/50) is 3.1 decades, which is broader than the half-width of 2.5 decades for the corresponding theoretical curve. This can be ascribed to the local heterogeneity, and the correlation length of the heterogeneity is similar to or longer than the size of the segments. We also note in Figures 7 and 8 that the  $\epsilon''$  curve after subtraction of the contribution of the normal mode is broader on the low-frequency side than on the high-frequency side. This trend is the reverse of ordinary behavior and can be

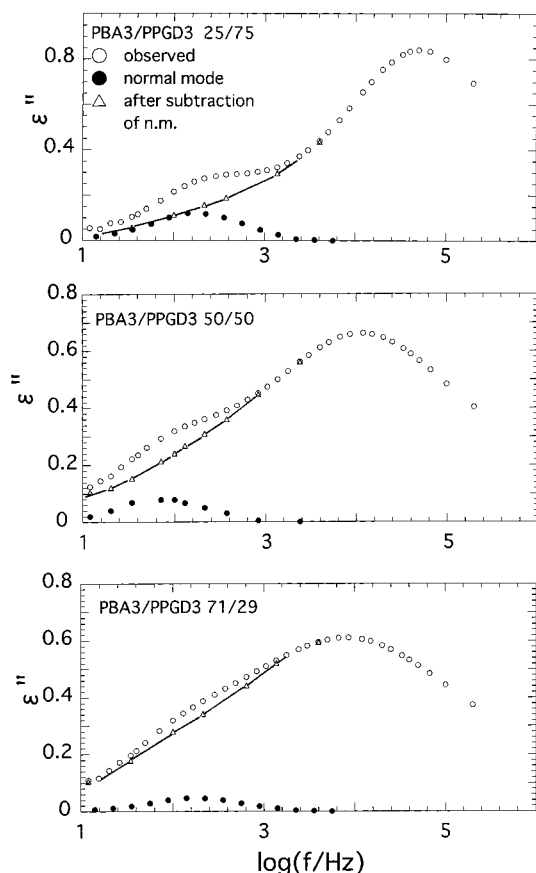


**Figure 7.** Resolution of  $\epsilon''$  curves for PBA-3/PPGD-3 blends into the contributions of the segmental mode ( $\Delta$ ) and the normal mode ( $\bullet$ ). Open circles are observed  $\epsilon''$  curves at 231 K.

explained by assuming a Gaussian distribution of concentration fluctuations, as discussed later.

As mentioned above, the normal mode does not change in blends, indicating that the correlation length is less than the end-to-end vector of the PPG chains. The linear PPG used in this study is a bifurcated chain in which the direction of the parallel component of the dipoles is inverted at the center of the molecule.<sup>5</sup> Thus, the normal mode of PPGD-3 corresponds to the second normal mode of the Rouse theory<sup>26</sup> and reflects the fluctuation of the distance  $R$  between chain end and the center of the chain. In the case of star-shaped PPGT-6, the normal mode reflects the fluctuation of the distance  $R$  between the chain end and the junction point.<sup>8,27</sup> It is reported that the  $\langle r^2 \rangle_0/M$  for the unperturbed PPG chain is  $0.00735 \text{ nm}^2/\text{g}$ .<sup>22</sup> Using this value, we obtain  $R = 3.3 \text{ nm}$  for PPGD-3 and  $R = 3.8 \text{ nm}$  for PPGT-6. Thus, the correlation length of concentration fluctuation is less than ca. 3 nm.

Now we test the blending rule given by eq 3 in more detail. Two discrepancies between the observed and calculated  $\epsilon''$  curves can be recognized. First, the observed main peak is broader than the calculated one as pointed out above. Second, a discrepancy is seen in the separation  $\Delta_\omega$  of the normal mode and the main peak measured along the  $\log f$  axis. As is seen in Figures 7 and 8, the observed  $\Delta_\omega$  is shorter than the calculated one and decreases with increasing PBA-3 content.

In the formulation of eq 3, we assumed a common friction  $\zeta_b$  for both components. If  $\zeta_b$  for the PPG molecules ( $\zeta_b^{\text{PPG}}$ ) is slightly lower than that of PBA ( $\zeta_b^{\text{PBA}}$ ), the present results may be explained qualita-



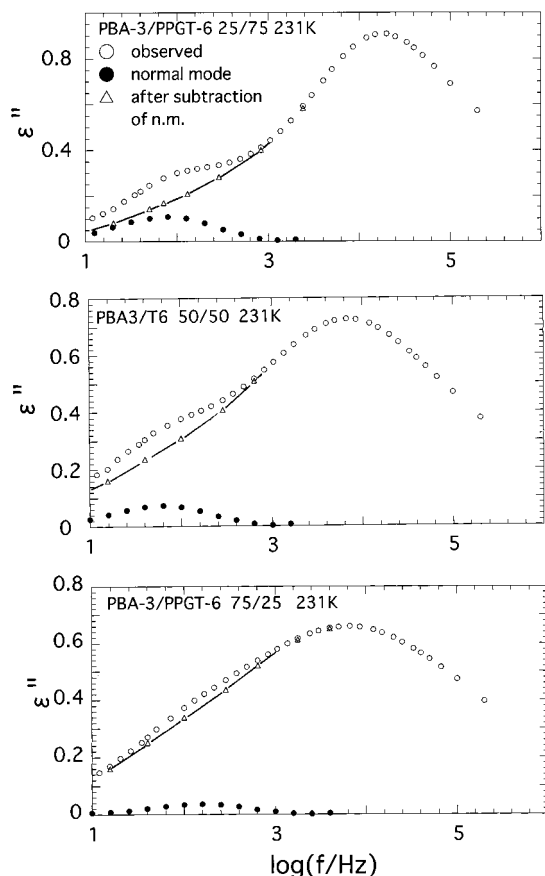


**Figure 8.** Resolution of  $\epsilon''$  curves for PBA-3/PPGT-6 blends into the contributions of the segmental mode ( $\Delta$ ) and the normal mode ( $\bullet$ ). Open circles indicate observed  $\epsilon''$  curves at 231 K.

tively. On the basis of this view, eq 3 was modified so that PBA and PPG have different  $\zeta_b$ , and the composite curves were calculated considering  $\zeta_b^{\text{PPG}}$  as an adjustable parameter. However, we could not realize the  $\epsilon''$  curves having a smaller  $\Delta_\omega$ . This is because the peak for the segmental mode of PPG is relatively sharp, and hence  $\Delta_\omega$  of the composite curve changes little for any values of  $\zeta_b^{\text{PPG}}$ . To explain  $\Delta_\omega$  on the basis of this model, we have to use the  $\epsilon''$  curve of PPG having a much broader distribution of relaxation times than that given in Figure 5.

Previously, Adachi et al.<sup>28</sup> reported for concentrated toluene solutions of *cis*-polyisoprene (PI) that  $\Delta_\omega$  decreased with decreasing PI concentration  $C$  (in w/v) and  $\Delta_\omega \sim 2 \log C$ . Figure 9 shows the plots of  $\Delta_\omega$  vs content of PPG. In this figure, we see that the slope is close to 2 and the behavior is very similar to PI solution. For toluene solutions of PI, this behavior was explained by assuming that the size of the unit for the segmental motion increases with decreasing concentration.<sup>28</sup> Since segmental motions can be regarded as the elementary process for the large scale motions, the size of the segment results in the decrease of the number of subunits in the chain. Thus, the separation between the segmental and normal modes becomes shorter. If this explanation is applicable to the present blends, PBA-3 is regarded as a solvent for the PPG molecules. It is interesting to test whether this relation also holds for blends composed of high molecular weight PBA. In PBA-21/PPG blends,  $\Delta_\omega$  is almost independent of concentration (see Figures 13 and 14). However, as discussed later, PBA-21/PPG blends appear to be locally segre-

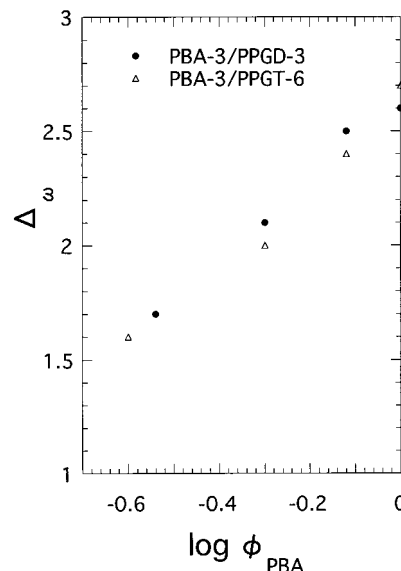


**Figure 9.** Dependence of the separation  $\Delta$  between the loss peaks for the segmental mode (sm) and the normal mode (nm) on the content of PBA. Here  $\Delta$  is defined by  $\Delta = \log f_m(\text{sm}) - \log f_m(\text{nm})$ .

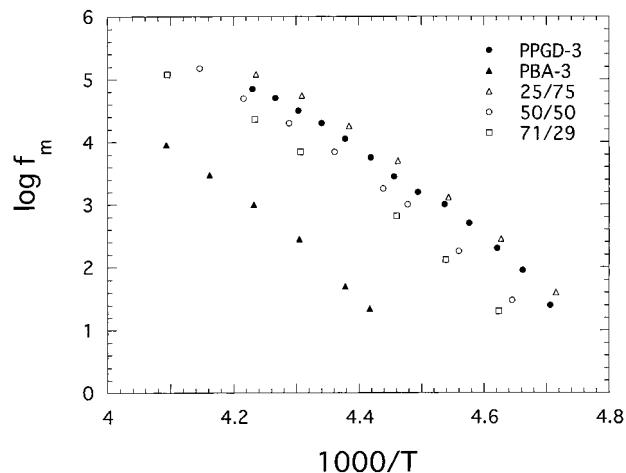


**Figure 10.** Arrhenius plots of the loss maximum frequency  $f_m$  for the segmental mode of PBA-3/PPGD-3 blends.

gated, and hence we should be careful about concluding that  $\Delta_\omega$  becomes independent of  $w$  when the molecular weight of PBA is high. To summarize, the concentration dependence of  $\Delta_\omega$  in PBA/PPG blends remains as a future problem.

**Comparison of Linear and Star-Shaped PPG.** In part 1 we speculated that the PBA segments do not contact with the segments of star-shaped PPG at the center of the molecule.<sup>1</sup> If this is the case, the segmental mode should split into two modes, due to almost pure PPG and due to the mixed parts. Furthermore, the normal mode will become broader since the mobility of the subchains at the central part differs from that at the chain ends.<sup>29</sup> However, as seen in Figures 7 and 8, the main peak in PBA-3/PPGT-6 blends is unimodal, and its shape is very close to that of PBA-3/PPGD-3. Therefore, strong segregation in PBA-3/PPGT-6 blends as speculated in part 1 must be ruled out.

**Blending Rule for Friction Coefficients.** The blending rule eq 3 for a mixed blend assumes a common friction coefficient  $\zeta_b$  which controls the cooperative motions of both components. Thus,  $\zeta_b$  is proportional to the relaxation time  $\tau_s$  for the segmental motions in the

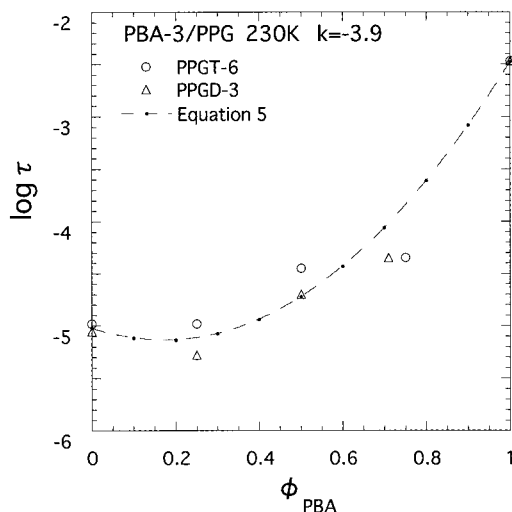


**Figure 11.** Dependence of relaxation time  $\tau$  on PBA-3 content in blends of PBA-3/PPGD-3 and PBA-3/PPGT-6 at 230 K. This figure represents the dependence of friction coefficient  $\zeta$  on PBA-3 content since  $\zeta$  is proportional to  $\tau$ . Dashed line represents eq 5 with arbitrary shifts along the ordinate.

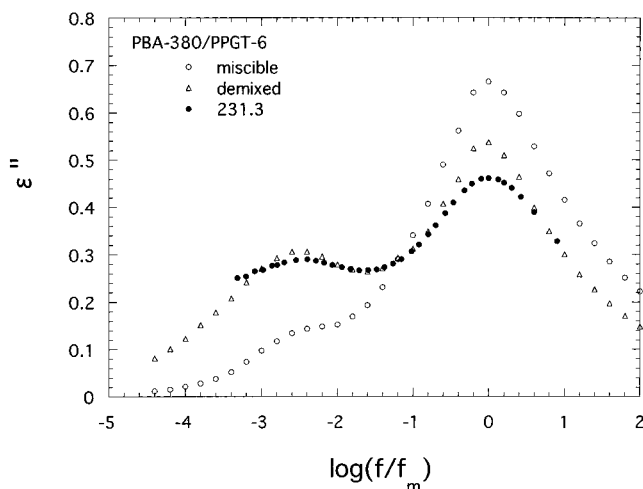


**Figure 12.** Comparison of the observed  $\epsilon''$  curve of PBA-380/PPGT-6 at 231 K with theoretical curves calculated with eq 1 for the demixed state and eq 3 for mixed state.

blend. Figure 10 shows the Arrhenius plots of  $\log f_m (=1/(2\pi\tau_s))$  versus inverse of temperature  $1/T$  for the PPGD-3/PBA-3 blends and those for the pure components. It is seen that the values of  $f_m$  of blends are close to that of PPG over a wide range of composition. When the concentration  $w$  of PBA-3 is 0.7, the Arrhenius plot is approximately intermediate to those of pure PBA and PPG. Similar behavior was also observed for the PPGT-6/PBA-3 blends. This behavior can be recognized more clearly in Figure 11 where the dependence of the relaxation time  $\tau_s$  on the content  $w_{PBA}$  of PBA-3 is shown for blends of PBA-3/PPGD-3 and PBA-3/PPGT-6 at 230 K. It is seen that  $\tau_s$  and hence  $\zeta_b$  are almost independent of the composition in the range of  $w_{PBA} < 0.5$  but changes steeply in the range  $w_{PBA} > 0.7$ .

We may express the blending rule for friction coefficient  $\zeta$  in a blend composed of polymers 1 and 2 as

$$\ln \zeta_b = w \ln \zeta_1 + (1 - w) \ln \zeta_2 + kw(1 - w) \quad (5)$$

where  $w$  is the concentration of either component. The last term is the correction term due to the interactions of 1 and 2. The negative  $k$  indicates repulsive interac-

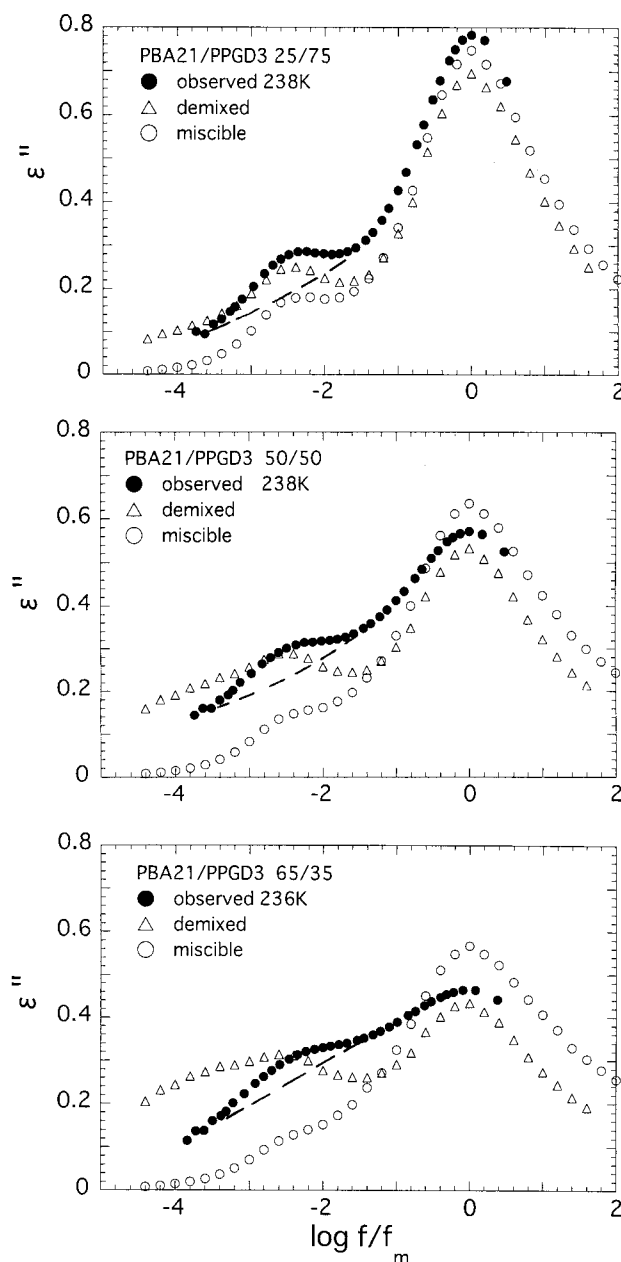


**Figure 13.** Comparison of the observed  $\epsilon''$  curve of PBA-21/PPGD-3 at 231 K with theoretical curves calculated with eq 1 for the demixed state and eq 3 for mixed state. (Top) blend with composition of 25/75, (middle) 50/50, (bottom) 65/35.

tions between the components and causes an increase of free volume by blending, and vice versa. When the size of the region of cooperative motions is  $a$ ,  $\tau_s$  is proportional to  $\zeta a^3$ . Therefore, this equation also holds for  $\tau_s$  when  $a$  is independent of the composition. Even if the size  $a$  changes with composition,  $\tau_s$  of blends can be given by an equation very similar to eq 5. The dashed line in Figure 11 represents eq 5 calculated with  $k = -3.9$ . The negative sign of  $k$  is consistent with the positive interaction parameters  $\chi$  for PBA/PPG blends reported in part 1.<sup>1</sup>

**Dielectric Behavior of Phase-Separated State.** Figure 12 shows the  $\epsilon''$  curves of the PBA-380/PPGT-6 (50/50) blend which is in the phase-separated state at temperatures of the dielectric measurements. From the phase diagram reported in part 1, this blend is separated into almost pure PPGT-6 and a PBA-rich phase having the composition of PBA/PPG  $\sim 90/10$ . The

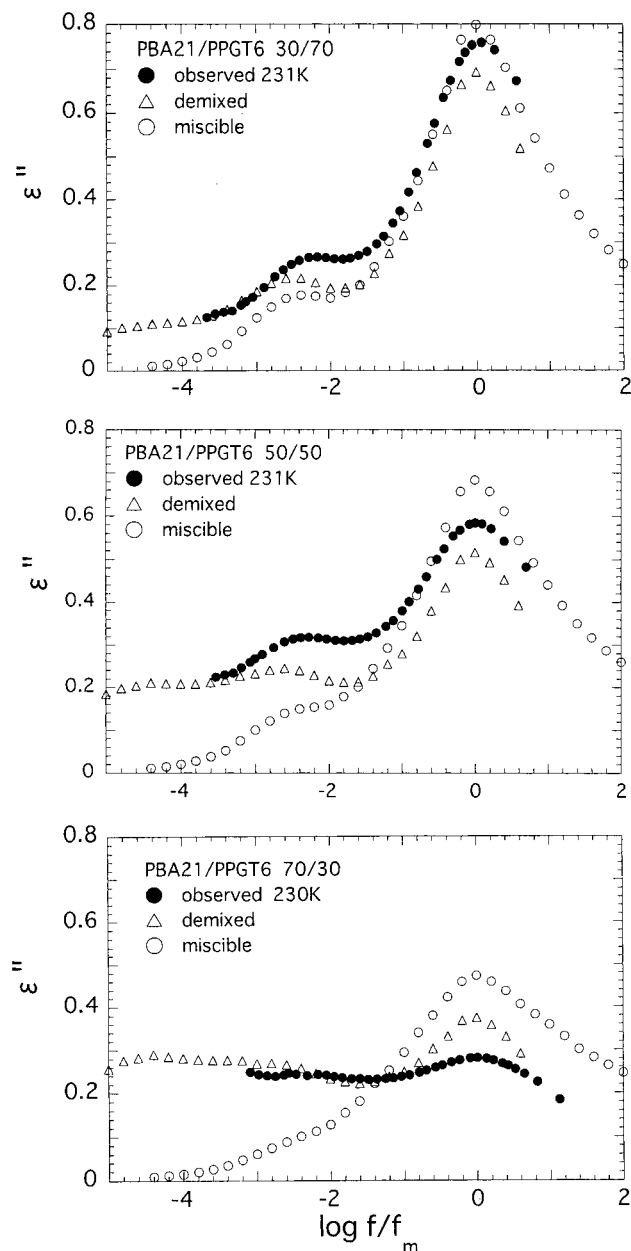


**Figure 14.** Comparison of the observed  $\epsilon''$  curve of PBA-21/PPGT-6 at 231 K with theoretical curves calculated with eq 1 for the demixed state and eq 3 for mixed state. (Top) blend with composition of 25/75, (middle) 50/50, (bottom) 70/30.

volume fractions of the PBA-rich and PPG-rich phases are ca. 0.6 and 0.4, respectively. In Figure 12 the observed  $\epsilon''$  curve is compared with the curves calculated with eqs 1 and 3 corresponding to completely demixed and mixed states, respectively. It is seen that in the low-frequency region that the observed curve agrees well with the theoretical curve for the demixed state. In the region of the main peak, the observed peak height is lower than the calculated one and the observed peak is broad. The PBA-rich phase contains ca. 10% of PPGT-6, and probably there exists a heterogeneity which results in a broad main peak.

**Dielectric Behavior near the Cloud Point.** In part 1 the phase diagrams of PBA21/PPGD-3 and PBA-21/PPGT-6 blends have been estimated. The cloud points of these blends locate near temperatures of dielectric measurements. Specifically for PBA-21/PPGD-3 blends, the cloud points at 25/75, 50/50, and 65/35 compositions

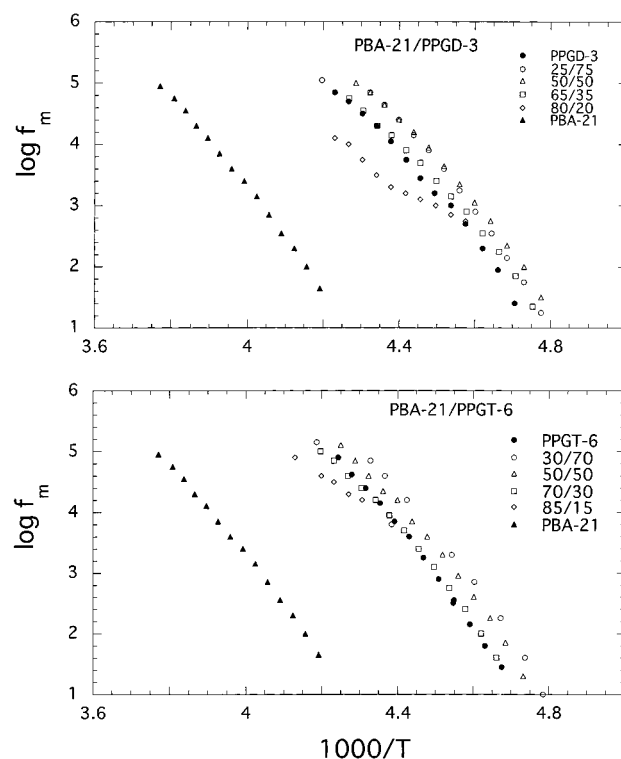


**Figure 15.** Arrhenius plots of the loss maximum frequency  $f_m$  for the segmental mode of PBA-21/PPGD-3 blends (top) and those for PBA-21/PPGT-6 blends (bottom).

are 245, 240, and 225 K, respectively, and for PBA-21/PPGT-6 blends, the cloud points at 30/70, 50/50, and 70/30 compositions are 265, 262, and 245 K, respectively. It was expected before the dielectric measurements were conducted that the  $\epsilon''$  curves of PBA-21/PPGD-3 blends would change from that given by eq 1 to that given by eq 3 at the cloud points. However, as shown in Figure 2, the shape of the  $\epsilon''$  curves of PBA-21/PPGD-3 blends did not change, and they were approximately superposable. Two loss peaks are separated clearly compared with the  $\epsilon''$  curves for the mixed blends shown in Figures 1, 7, and 8. The intensity of the low-frequency peak is too high to be attributed to the normal mode of PPG (shown in Figure 5), and therefore it is due to both the segmental mode of PBA-21 and the normal mode of PPGD-3. This indicates that PBA-21/PPGD-3 blends are weakly segregated even at temperatures above the cloud point.

The  $\epsilon''$  curves of PBA-21/PPGD-3 blends at about 238 K are compared with the mixing rules given by eqs 1 and 3 (Figure 13). It is seen that the observed curve is intermediate to the theoretical curves given by eqs 1 and 3. The  $\epsilon''$  curve after subtraction of the normal mode (dashed line) still has a broad shoulder in the lower frequency side of the main peak. Especially we note that the  $\epsilon''$  curve at 65/35 composition exhibits a broad shoulder of the low-frequency side even though it was observed above the cloud point (225 K). Obviously, this is due to the contribution of the PBA chains which have a lower mobility than the PPG molecules.

Figure 14 compares the observed and theoretical  $\epsilon''$  curves at about 230 K for PBA-21/PPGT-6 blends. For a blend of 50/50 composition we see that the  $\epsilon''$  curve is intermediate to the  $\epsilon''$  curves for the mixed and demixed states, as observed for the PBA-21/PPGD-3 blend. However, the observed curve is closer to the curve corresponding to the demixed state. We also note that

in a blend of 70/30 composition the  $\epsilon''$  curve becomes very broad. Probably this blend is phase separated, and the two phases have a strong heterogeneity. The Arrhenius plots for the main peaks of these blends are shown in Figure 15. It is seen that the plots for the blends are close to that of PPG over wide concentration range. This behavior is different from the behavior of mixed blend shown in Figure 10. This also indicates that the blends are in a weakly segregated state, and the relatively sharp  $\epsilon''$  peak of PPG becomes the main peak at any composition.

The above-mentioned results for PBA-21/PPG blends may be interpreted as follows. First, it is noted that the distribution of molecular weight of PBA-21 is not very sharp ( $M_w/M_n = 1.27$ ), and therefore the blends may exhibit relatively broad distribution of phase separation temperature. We also note that, even in phase-separated states, there exists an interphase and the thickness of the interphase is expected to be broad since the difference of free energy between two phases is small near the cloud point. Furthermore, the domain size is of the order of micrometers, and hence the area of interface is large. These factors may act equally so that the dielectric spectra of the blends become broad.

**Concentration Fluctuation and Distribution of Relaxation Times of the Segmental Mode.** We return to miscible blends and consider the effect of heterogeneity on the distribution of relaxation times for the segmental mode. We have concluded that the correlation length  $\xi$  for PBA-3/PPGD-3 and PBA-3/PPGT-6 blends is less than 3 nm. Zetsche and Fischer<sup>9</sup> proposed that mixed blends have a Gaussian distribution of concentration fluctuation. This was tested in terms of the dielectric method by Katana et al.<sup>10</sup> Recently, Yada et al.<sup>30</sup> reported dielectric measurements on concentrated solution of poly(vinyl acetate) near the glass transition temperature and explained the distribution of relaxation times by assuming a Gaussian distribution of concentration. In this section we test whether the  $\epsilon''$  curves of the present blends can be explained by this model.

We assume that concentration fluctuation in a blend composed of polymers 1 and 2 can be represented by a Gaussian distribution:

$$P(\phi) = P_0 \exp[-(\phi - \phi_0)^2/(2\sigma)] \quad (6)$$

where  $\phi$  is the local concentration of the component 1,  $P(\phi)$  the distribution function, and  $\phi_0$  the average concentration of component 1. The parameter  $\sigma$  is equal to the mean-square fluctuation of local concentration  $\langle(\phi - \phi_0)^2\rangle$  in a volume of  $\xi^3$ . Since the relaxation time varies with concentration, the distribution of local concentration  $\phi$  causes the distribution of relaxation times  $g(\ln \tau)$ . Here, we may assume that the dependence of  $\ln \tau$  on  $\phi$  is given by eq 5. From eqs 5 and 6, we express the distribution function  $g(\ln \tau)$  of relaxation times. Then the dielectric loss curve is given by a form

$$\epsilon'' = \int_{-\infty}^{\infty} g(\ln \tau) \Psi(\omega, \tau) d \ln \tau \quad (7)$$

where  $\Psi(\omega, \tau)$  is the normalized loss curve for a blend in which there is no concentration fluctuation. We assumed that  $\Psi(\omega, \tau)$  is given by the Havriliak–Negami equation (eq 4) for the segmental mode of pure PPGD-3. The best fit  $\epsilon''$  curves for PBA-3/PPGD-3 (50/50) and (71/29) blends are shown in Figure 1 by the dotted lines.

As is seen in this figure, the calculated curve reproduces well the asymmetrical shape of the  $\epsilon''$  curve having slightly broader distribution in the low-frequency side. This is because, although the Gaussian distribution of concentration is symmetrical around the average concentration, the concentration dependence of the relaxation time  $d \log \tau / d\phi$  becomes steep in the PBA-rich region as shown in Figure 11. The parameters  $\sigma$  ( $=\langle(\phi - \phi_0)^2\rangle$ ) used in this calculation are 0.083 for 50/50 composition and 0.049–0.141 for 71/29 composition. For 71/29 composition,  $\sigma$  increases with decreasing temperature. These data indicate that the concentration fluctuations  $\langle(\phi - \phi_0)^2\rangle^{1/2}$  in these blends are 0.2–0.3 g/cm<sup>3</sup>.

## Conclusions

Dielectric relaxations of PBA/PPG blends have been observed in the temperature range from 210 to 250 K. We have found that the dielectric behavior of a PBA/PPG blend depends strongly on the separation between the cloud point and the temperature of dielectric measurements. To analyze the dielectric data, we have assumed two blending rules for the complex dielectric constant  $\epsilon^*$  in the mixed and demixed states. These rules are found to be useful as a working hypothesis for the analyses of the dielectric data of blends. The dielectric normal mode relaxation of PPG is clearly observed for blends. The normal mode does not change its spectrum in miscible blends, indicating that the correlation length  $\xi$  of concentration fluctuation is less than the end-to-end vector of ca. 3 nm for the PPG molecules used in this study. On the other hand, the loss curve for the segmental mode becomes broad, indicating that  $\xi$  is similar to or longer than the size of the segments. For mixed blends, the broadening of dielectric relaxation spectra can be explained on the basis of a Gaussian distribution of concentration fluctuations. It has been found that the separation of the loss peaks for the normal and segmental modes decreases with increasing content of PBA. Explanation of this behavior remains as a future problem. Remarkable differences in dielectric behavior between the blends containing linear PPG and star-shaped PPG are not seen, indicating that the concentration fluctuations in blends of linear PPG are similar to those of star-shaped PPG. Blends composed of PPG and high molecular weight PBA are in the phase-separated state and exhibit  $\epsilon''$  curves conforming approximately to the blending rule for the demixed state. For blends having cloud points near temperature of measurements, the  $\epsilon''$  curve exhibits its intermediate behavior compared to the  $\epsilon''$  curves predicted by the blending rules for the mixed and demixed states.

## References and Notes

- (1) Hayakawa, T.; Adachi, K. *Macromolecules* **2000**, *33*, 6834.
- (2) Flory, P. J. *J. Chem. Phys.* **1941**, *9*, 660.
- (3) Huggins, M. L. *J. Chem. Phys.* **1941**, *9*, 440.
- (4) Se, K.; Takayanagi, O.; Adachi, K. *Macromolecules* **1997**, *30*, 4877.
- (5) Stockmayer, W. H. *Pure Appl. Chem.* **1967**, *15*, 539.
- (6) Adachi, K.; Kotaka, T. *Prog. Polym. Sci.* **1993**, *18*, 585.
- (7) Baur, M. E.; Stockmayer, W. H. *J. Chem. Phys.* **1965**, *41*, 4311.
- (8) Stockmayer, W. H.; Burke, J. J. *Macromolecules* **1969**, *2*, 647.
- (9) Zetsche, A.; Fischer, E. W. *Acta Polym.* **1994**, *45*, 168.
- (10) Katana, G.; Fischer, E. W.; Hack, Th.; Abetz, V.; Kremer, F. *Macromolecules* **1995**, *28*, 2714.
- (11) Runt, J. P. Dielectric Studies of Polymer Blends. In *Dielectric Spectroscopy of Polymeric Materials*; Runt, J. P., Fitzgerald,



- J. J., Eds.; American Chemical Society: Washington, DC, 1997; Chapter 10, pp 283–302.
- (12) Alegria, A.; Colmenero, C. M.; Ngai, K. L.; Roland, C. M. *Macromolecules* **1994**, *27*, 4486.
- (13) Wetton, A. G.; MacKnight, W. J.; Fried, J. R.; Karasz, F. E. *Macromolecules* **1978**, *11*, 158.
- (14) Shears, M. S.; Williams, G. *J. Chem. Soc., Faraday Trans.* **1973**, *69*, 608.
- (15) Wagner, K. W. *Arch. Elektrotechnol.* **1914**, *2*, 371.
- (16) Sillars, R. W. *J. Inst. Electron. Eng.* **1937**, *80*, 378.
- (17) Bottcher, C. J. F.; Bordewijk, P. *Theory of Electric Polarization*; Elsevier: Amsterdam, 1978; Vol. I.
- (18) Onsager, L. *J. Am. Chem. Soc.* **1936**, *58*, 1486.
- (19) Kirkwood, J. G. *J. Chem. Phys.* **1939**, *7*, 911.
- (20) Diaz-Calleja, R.; Riande, E. In *Dielectric Spectroscopy of Polymeric Materials*; Runt, J. P., Fitzgerald, J. J., Eds.; American Chemical Society: Washington DC, 1997; Chapter 5, pp 139–173.
- (21) Schallamach, A. *Trans. Faraday Soc.* **1946**, *42A*, 180.
- (22) Hill, N. E.; Vaughan, W. E.; Price, A. H.; Davies, M. *Dielectric Properties and Molecular Behaviour*; van Nostrand Reinhold: New York, 1969; pp 340–344.
- (23) Rellick, G. S.; Runt, J. *J. Polym. Sci., Polym. Phys. Ed.* **1986**, *24*, 313.
- (24) *Polymer Handbook*, 3rd ed.; Brandrup, J., Immergut, E. H., Eds.; John-Wiley: New York, 1989.
- (25) Havriliak, S.; Negami, S. *Polymer* **1967**, *8*, 161.
- (26) Rouse, P. E. *J. Chem. Phys.* **1953**, *21*, 1272.
- (27) Ham, J. S. *J. Chem. Phys.* **1957**, *26*, 625.
- (28) Adachi, K.; Imanishi, Y.; Kotaka, T. *J. Chem. Soc., Faraday Trans. 1* **1989**, *85*, 1083.
- (29) Stockmayer, W. H.; Kennedy, J. W. *Macromolecules* **1975**, *8*, 351.
- (30) Yada, M.; Nakazawa, M.; Urakawa, O.; Morishima, Y.; Adachi, K. *Macromolecules*, in press.

MA000685N